



Article

# Friction Stir Spot Welding of Thin Aluminium Sheets to Polyamide 6: A Study of the Welding Parameters and Strategies

Miguel A. R. Pereira <sup>1</sup>, Ivan Galvão <sup>1,2</sup>, José Domingos Costa <sup>1</sup>, Rui M. Leal <sup>1,3</sup> and Ana M. Amaro <sup>1,\*</sup>

- <sup>1</sup> University of Coimbra, CEMMPRE, ARISE, Department of Mechanical Engineering, Rua Luís Reis Santos, 3030-788 Coimbra, Portugal; miguel.reis.pereira@dem.uc.pt (M.A.R.P.); ivan.galvao@isel.pt (I.G.); jose.domingos@dem.uc.pt (J.D.C.); rui.leal@ipleiria.pt (R.M.L.)
- <sup>2</sup> UnIRE, ISEL, Polytechnic University of Lisbon, Rua Conselheiro Emídio Navarro, 1, 1959-007 Lisboa, Portugal
- <sup>3</sup> LIDA-ESAD.CR, Instituto Politécnico de Leiria, Rua Isidoro Inácio Alves de Carvalho, 2500-321 Caldas da Rainha, Portugal
- \* Correspondence: ana.amaro@dem.uc.pt

**Abstract:** The joining of aluminium alloy AA6082-T6 to polyamide 6 (PA6) by friction stir spot welding (FSSW) was investigated in the current work. Although previous studies can be found on the joining of polymers and metals by FSSW, welding using aluminium plates as thin as the ones used in this work (1 mm) was not found. The influence of the plunge depth (0.1 to 0.5 mm) and the dwell time (15 and 30 s) parameters on the welding results was studied. In general, the increase of these parameters led to the improvement of the maximum load of the joints under tensile-shear testing. Additionally, the feasibility of multiple spot welding was tested and proven. Finally, although most of the welds were performed with a pinless tool, a tool with a conical pin and a concave shoulder was used for comparison. The use of this more conventional tool resulted in joints easily broken by handling. Still, the potential of the conical pin tool was demonstrated. The different conditions were evaluated based on morphology and tensile-shear testing. The weld with the best mechanical behaviour was produced with multiple spot welding, which failed for a maximum load of about 2350 N.

**Keywords:** friction stir spot welding (FSSW); hybrid structure; aluminium alloy; polyamide 6 (PA6); welding parameters



**Citation:** Pereira, M.A.R.; Galvão, I.; Costa, J.D.; Leal, R.M.; Amaro, A.M. Friction Stir Spot Welding of Thin Aluminium Sheets to Polyamide 6: A Study of the Welding Parameters and Strategies. *J. Compos. Sci.* **2024**, *8*, 21. <https://doi.org/10.3390/jcs8010021>

Academic Editors: Francesco Tornabene and Thanasis Triantafyllou

Received: 31 October 2023  
Revised: 20 December 2023  
Accepted: 29 December 2023  
Published: 8 January 2024



**Copyright:** © 2024 by the authors. Licensee MDPI, Basel, Switzerland. This article is an open access article distributed under the terms and conditions of the Creative Commons Attribution (CC BY) license (<https://creativecommons.org/licenses/by/4.0/>).

## 1. Introduction

Two major concerns of today's society are the improvement of energy efficiency and the reduction of pollutant gas emissions, especially in the transport sector. Reducing the weight of the vehicles is one of the best solutions to achieve this goal [1–3]. With this objective in mind, the replacement of conventional all-metal structures by hybrid structures composed of lightweight metal alloys and polymer-based materials has been attracting more and more interest. Nevertheless, the number of applications ends up being limited due to the difficulty in efficiently joining these materials with such different characteristics [4].

Mechanical fastening and adhesive bonding are the two main methods traditionally used for this purpose, although they present several disadvantages. For example, mechanical fastening uses mechanical components that add unnecessary weight to the structures and the adhesives are normally susceptible to thermal and environmental degradation [5]. As a result, the need to find alternative methods to join polymer-based materials and lightweight metal alloys becomes evident.

One of the methods that can be used to join metals and polymers is friction stir welding (FSW). The FSW is a joining process initially developed to overcome the difficulties of aluminium welding. Patented in 1991 in The Welding Institute by Thomas et al. [6,7], it has been used not only to join aluminium but also to weld other metals, polymers, and composites [8]. Furthermore, the FSW is a process that allows the joining of dissimilar

materials [9–11]. The friction stir spot welding (FSSW) is an FSW variant for spot joining and, therefore, differs from the base process as there is no translation movement of the tool. The FSW/FSSW process works by penetrating a non-consumable rotating tool at a relatively high rotational speed, which generates heat through friction and severe plastic deformation, allowing the welding of the adjoining surfaces.

The feasibility of joining aluminium alloys to non-reinforced polymers by FSSW has already been demonstrated in several studies. Most authors use pinless tools and an overlap joint configuration with the aluminium placed over the polymeric material. The improvement of the joint quality and strength has been studied not only by the optimization of the main welding parameters, such as rotational speed, plunge depth [12,13], axial force [14–16], and dwell time [14–16] but also by testing different surface treatments on the aluminium side in contact with the polymer. These surface treatments improve the micro-mechanical interlocking of the materials [17,18], by allowing a better entrapment of the polymer in the metal rugosities [18,19]. The main surface treatments reported in previous works are grinding [20], sandblasting [19], chemical etching [13], laser texturing [14,15,21], plasma electrolytic oxidation [22,23], and anodizing pre-treatment [24].

The joining of thin sheets of aluminium alloy AA6082-T6 to polyamide 6 (PA6) using FSSW was investigated in this work. Although there is already some published literature reporting the joining of polymers and metals by FSSW, welding using aluminium plates as thin as the ones used in this work (1 mm) was not found. Furthermore, the influence of plunge depth and dwell time parameters on joint quality and strength as well as the feasibility of multiple spot welding were studied. Although not often referred to in the literature, multiple-spot welding has more industrial applications than single-spot welding [25]. Finally, the pinless tool used in most of the welding tests was compared to a more conventional tool, which is composed of a conical pin and a concave shoulder. The comparison between the different conditions was based on a morphological analysis of the top surface and cross-section of the welds and the mechanical performance of the joints.

## 2. Materials and Methods

The materials used in this work were 1 mm thick aluminium alloy AA6082-T6 and 6 mm thick PA6. The chemical composition of this aluminium alloy is shown in Table 1, and the mechanical, physical, and thermal properties of both materials are shown in Table 2. Tables 1 and 2 were built based on information provided by the supplier and experimental tests.

**Table 1.** Chemical composition of the aluminium alloy AA6082-T6.

Material	Si	Fe	Cu	Mn	Mg	Cr	Zn	Ti	Al
AA6082-T6	0.7–1.3	<0.5	<0.1	0.4–1	0.6–1.2	<0.25	<0.2	<0.1	Balance

**Table 2.** Mechanical, physical and thermal properties of the AA6062-T6 and the PA6.

Property	AA6082-T6	PA6
Density (g/cm <sup>3</sup> )	2.70	1.14
Ultimate tensile strength (MPa)	290–310	55 *
Yield Strength (MPa)	250–260	38 *
Vickers Microhardness (HV)	103 *	5.8–6.8 *
Thermal conductivity (W/K.m)	150–180	0.28
Melting temperature (°C)	550–650	220
Elongation at break (%)	10	170 *

\* Properties obtained experimentally.

The welds were prepared with a lap joint configuration, using 100 mm long and 40 mm wide plates and an overlap area of 40 × 40 mm<sup>2</sup>. Moreover, the aluminium plate was always positioned over the polymer plate and the welding was performed in the centre

of the overlapped area. Before assembly, the plates were cleaned with ethanol 96% vol. and dried with pressurised air. The aforementioned joint configuration is provided in Figure 1.

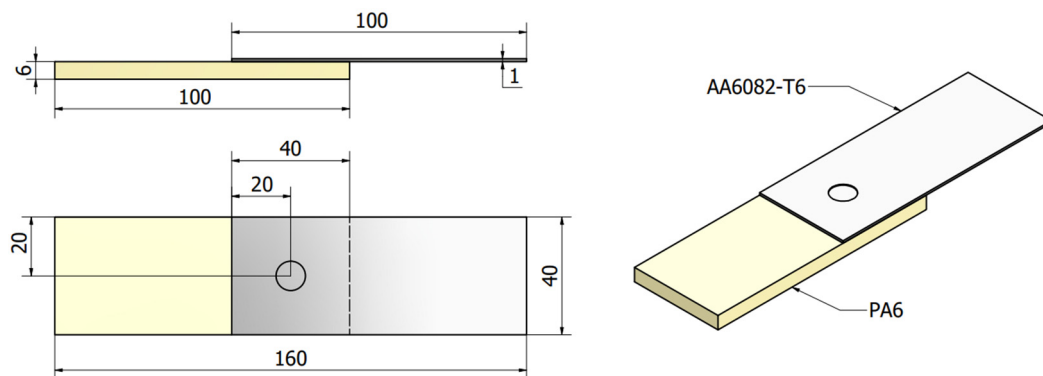


**Figure 1.** Joint configuration used during welding. Dimensions in mm.

Preliminary tests were carried out to study the influence of surface treatment of the aluminium side in contact with the polymer. The surface treatment consisted of dry grinding the aluminium surface using P100 SiC paper to increase its rugosity and remove the oxide layer and other impurities. These tests showed that when the aluminium surface is not treated, it detaches very easily from the polymer. In turn, the preliminary welds produced with the surface treatment of the aluminium significantly increased their strength due to the improvement of the mechanical interlocking mechanism.

Additionally, preliminary tests were also performed to study the influence of the tightening torque of the clamping frame, which fixes the materials to the working station, on the welding results. While the under-tightening of clamps led to misalignment of the assembly during welding, the over-tightening of the clamps led to severe deformation of the aluminium, promoting the free end to rise during welding, as represented in Figure 2a. As thin aluminium sheets were used, the rising of the free end resulted in the rupture of the aluminium under the tool from the rest of the plate, as can be seen in Figure 2b. As a result, both scenarios ultimately compromised the success of the welding process. By testing multiple conditions, it was found for this study optimum value of tightening torque of 25 N·m.

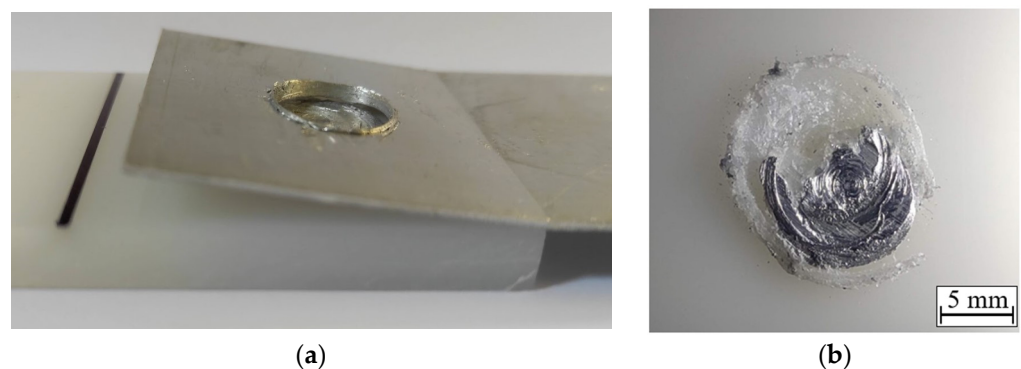


**Figure 2.** Welding results are promoted by excessive tightening of the clamping frame: (a) rise of the free end and (b) rupture of the aluminium under the tool.

The welding was performed on a milling machine using tungsten carbide tools and different tool geometries (TG). Although a pinless tool was used to perform most of the welding tests, part of them was carried out using a tool with a conical pin and concave shoulder for comparison. The pinless tool (PL) has a 10 mm in diameter shoulder and a flat bottom surface. In turn, the conical pin tool (CN) has a concave shoulder with a diameter

of 12 mm and a 1.3 mm long conical pin with 6 mm in diameter at the base and 3 mm in diameter at the tip. Both tools are illustrated in Figure 3.

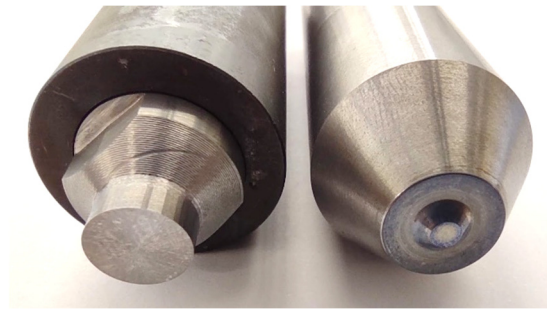


**Figure 3.** Welding tools used in this study: a pinless tool (left side) and a conical pin with a concave shoulder tool (right side).

Then, the influence of the dwell time (DT) and plunge depth (PD) was investigated. Dwell times of 15 and 30 s were compared, and the plunge depth was varied between 0.1 and 0.5 mm, at intervals of 0.1 mm. Furthermore, single-spot welding was compared to triple-spot welding to understand if the deformation of the aluminium plate during multiple-spot welding promoted the separation of the previously performed welds. All the different conditions experimented on are displayed in Table 3. The rotational speed used in all conditions was 1500 rpm. The choice of using this rotational speed was based on previous preliminary tests, where the rotational speed was varied between 870 and 2000 rpm.

**Table 3.** Protocol of the welding tests.

Designation *	Tool Geometry	Plunge Depth (mm)	Dwell Time (s)	Welding Spot Strategy
PL_0.1_15_S	Pinless	0.1	15	Single
PL_0.2_15_S	Pinless	0.2	15	Single
PL_0.3_15_S	Pinless	0.3	15	Single
PL_0.4_15_S	Pinless	0.4	15	Single
PL_0.5_15_S	Pinless	0.5	15	Single
PL_0.2_30_S	Pinless	0.2	30	Single
PL_0.2_15_T	Pinless	0.2	15	Triple
CN_0.2_10_S	Conical	0.2	10	Single

\* Nomenclature reasoning: TG\_PD\_DT\_Single (S) or Triple (T) Spot Welding.

Furthermore, during the preliminary tests, it was observed that the aluminium can easily stick to the shoulder. Consecutive welding tests without tool cleaning resulted in aluminium build-up, progressively changing the real tool geometry. This unintentional change in tool geometry cannot be controlled and can result in severe degradation of the aluminium plate. Figure 4 shows the surface finish of welds produced using the pinless tool without and with aluminium accumulation, Figure 4a,b, respectively, and the resulting cross-sections of these welds, Figure 4c,d, respectively. While a clean tool results in a smoother and more uniform weld surface (Figure 4a), when using a tool with aluminium accumulation the weld surface is much more irregular (Figure 4b). Additionally, from the cross-section of the welds it can be seen that a clean tool produces joints with a controlled deformation of the aluminium under the tool (Figure 4c), while the tool with material accumulation results in a severe deformation of the aluminium under the tool (Figure 4d). This more aggressive deformation favours the formation of cracks in the interior of the aluminium, as shown in Figure 4d. In order to ensure greater control of the welding parameters, the accumulation of material on the bottom of the tool was always checked before and after each weld, and cleaned if there was any stuck material.

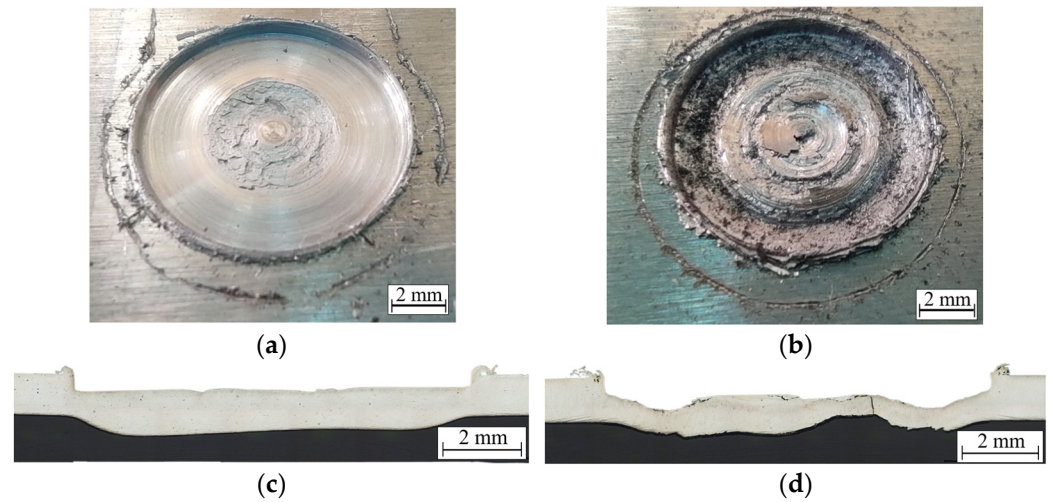


**Figure 4.** Weld surfaces produced using a tool (a) without and (b) with material accumulation and cross-sections of welds produced using a tool (c) without and (d) with material accumulation.

The different conditions were compared based on the weld morphology and mechanical performance. The morphological analysis resulted from the comparison of weld surfaces, transverse cross-sections and joining areas, using a Leica DM400M LED optical microscope. The morphological analysis was complemented with Scanning Electron Microscopy (SEM) images that were acquired using a ZEISS GeminiSEM 460 scanning electron microscope. In turn, the mechanical performance was based on tensile-shear testing, performed on a Shimadzu AGS-X universal tensile testing machine with a load capacity of 100 kN and using a deformation speed of 5 mm/min at room temperature. For the tensile-shear testing, 3 specimens were tested for each condition. To ensure that the solicitation was aligned, shim plates were used in the wedge grip areas.

### 3. Results

Figure 5a illustrates an example of a polymer-metal weld produced by FSSW using a pinless tool and Figure 5b shows the typical macrostructure of the weld cross-section. During welding, when the tool penetrates the aluminium, the metal under the shoulder is deformed and pushed against the polymer. Due to the frictional heat generated by the rotating tool, the temperature of the polymer close to the interface increases, causing the heated polymer to exhibit a fluid-like behaviour. Then, the aluminium pushed and deformed by the rotating tool easily penetrates the softened polymer, creating a macro-mechanical interlocking mechanism after cooling [17,18]. Due to heat conduction, the aluminium around the tool also significantly increases its temperature, consequently softening the polymer below it. The aluminium and the polymer are also joined in the region around the tool action zone by mechanical interlocking mechanisms. This is a possible reason why the welds performed on preliminary tests with untreated aluminium surfaces showed bad mechanical performance, as the smooth aluminium surfaces may not allow a good micro-mechanical interlocking due to the lack of roughness of the surfaces.

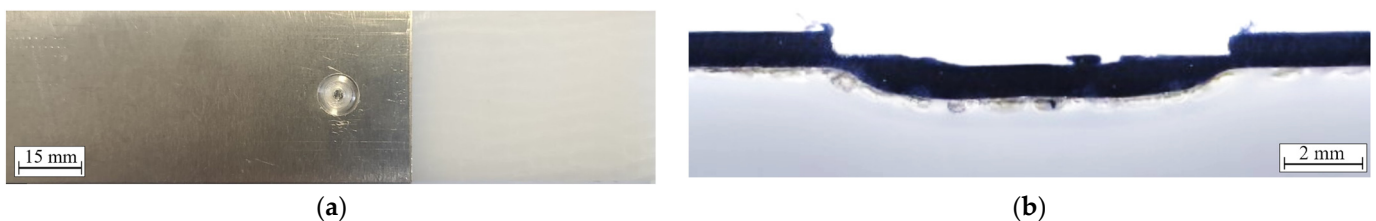


**Figure 5.** (a) Example of a polymer-metal weld produced by FSSW using a pinless tool and (b) a typical cross-section.

### 3.1. Plunge Depth

The plunge depth was the first parameter studied in this work. Penetrations ranging between 0.1 and 0.5 mm at intervals of 0.1 mm were tested and compared. The lowest plunge depth tested (PD = 0.1 mm) resulted in joints that could be easily separated by hand. Overall, the increase in plunge depth results in the increase of aluminium plunged into the polymer, which influences the joint strength. By increasing the penetration of the tool, it was possible to obtain effective joining for plunge depths of 0.2 (PL\_0.2\_15\_S), 0.3 (PL\_0.3\_15\_S) and 0.4 mm (PL\_0.4\_15\_S). Then, when using a plunge depth of 0.4 mm, cracks start to form in some welds due to excessive tool penetration, as shown in Figure 6. When the plunge depth was further increased to 0.5 mm, these cracks propagated, leading to the separation of the aluminium under the tool from the rest of the aluminium plate, and resulting in weld failure. Therefore, it can be concluded that increasing the plunge depth improves the mechanical performance of the joints up to the point where it leads to the breaking of the material under the tool.

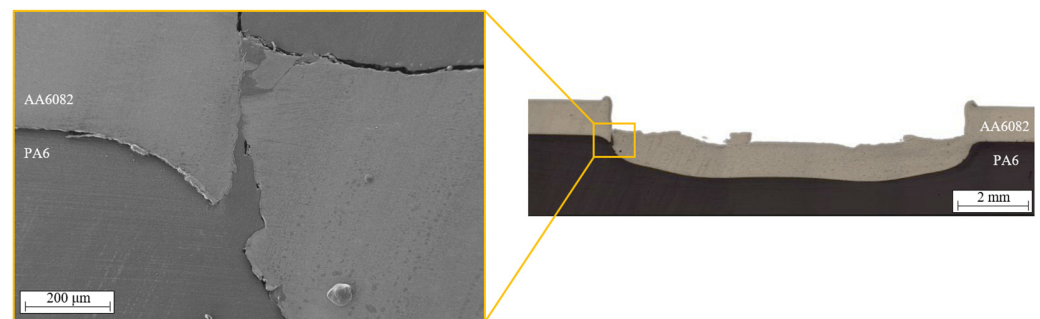


**Figure 6.** Cracking of the aluminium as a result of excessive tool penetration.

### 3.2. Dwell Time

After studying the influence of plunge depth on the FSSW process, the increase in dwell time from 15 s to 30 s was investigated. When the dwell time was increased, the materials were exposed for a longer period of time to the high temperatures of the process. Still, the dwell time did not affect the appearance of the weld surfaces since the surfaces of the two welds are similar to each other and the surface is illustrated in Figure 4a. On the other hand, by comparing the cross-sections of the welds produced with dwell times of 15 s (Figure 7a) and 30 s (Figure 7b), conditions PL\_0.2\_15\_S and PL\_0.2\_30\_S respectively, it can be observed that they display significant differences. The separation of the base material and the heat-affected polymer is identified in Figure 7a,b with dashed lines. In addition, the darker-coloured rounded structures indicate the presence of pores inside the polymer. Although both welds show the presence of pores in the polymer close to the interface, the increase in dwell time resulted in a significant increase in the size of the pores. More specifically, welds carried out with 15 s of dwell time resulted in pores up to approximately 1 mm wide, while welds carried out with 30 s of dwell time resulted in pores with a width ranging from approximately 2 mm to more than 5 mm. Additionally, the weld produced with a longer dwell time of 30 s (PL\_0.2\_30\_S) revealed a thicker layer of thermally affected polymer, with a maximum thickness in the weld centre of about 1.1 mm, while the weld produced with a shorter dwell time of 15 s (PL\_0.2\_15\_S) revealed a smaller layer with a maximum of about 0.6 mm, also in the central region. Due to the longer heat exposure, greater heating of the entire aluminium plate took place, allowing the heat to spread to a wider region, which promoted the formation of a larger joining area.



**Figure 7.** Cross sections of the weld conditions (a) PL\_0.2\_15\_S and (b) PL\_0.2\_30\_S.

As displayed in Figure 8, in terms of mechanical performance, the welds produced using the 15 s of dwell time (PL\_0.2\_15\_S) failed at a maximum force of about 1700 N, and the welds produced with a dwell time of 30 s (PL\_0.2\_30\_S) at 2100 N (highest values among the three specimens tested for each of these two conditions). The improvement of mechanical performance of about 24% was mainly attributed to the formation of a larger joining area. A longer dwell time increases the processing time of each weld, making the process less productive. However, these tests demonstrated that the increase in heat generation may result in an improvement in mechanical performance, despite leading to the formation of larger pore defects. At industrial and commercial levels, the dwell time must be as short as possible. In order to achieve similar results without increasing the process time, other strategies must be tested in the future, such as the increase of rotational speed or the use of larger tool diameters, for example.

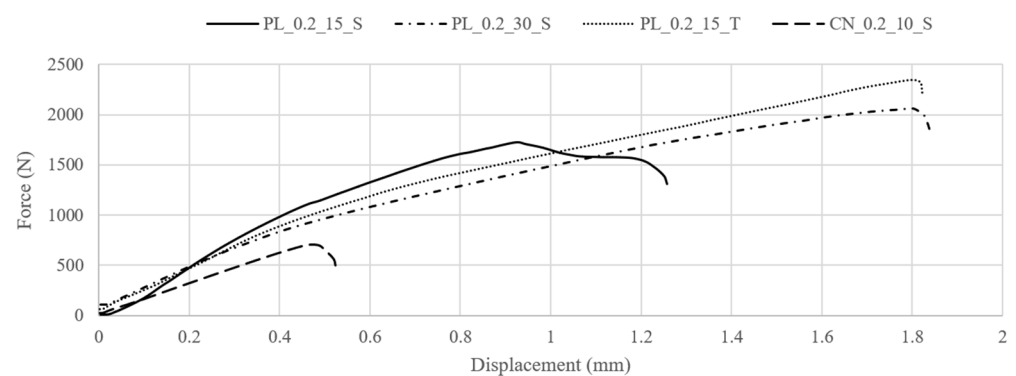


**Figure 8.** Force-Displacement curves for the specimen with the highest strength out of the three tested for each of the following conditions: PL\_0.2\_15\_S, PL\_0.2\_30\_S, PL\_0.2\_15\_T and CN\_0.2\_10\_S.

### 3.3. Triple Spot Welding

During welding, the aluminium around the tool action zone showed some deformation as a result of using thin metal plates. For this reason, single-spot welding, Figure 9a, was compared to triple-spot welding, Figure 9b, with the objective of understanding if the deformation associated with the production of multiple welding spots resulted in the detachment of the previous welds. The results showed that the multiple welding was successfully performed as the plates were still joined in each spot region after performing the three welding steps. Then, the mechanical performance was compared to understand if there was an improvement in joint strength. Figure 8 demonstrates that while the single spot weld failed at a maximum force of about 1700 N, the triple spot weld failed at 2350 N,

which represents an improvement of about 38%. It is important to note that because two welds were performed close to the border of the overlapped region in the triple spot weld, there was polymer extruded to the border of the joint. If the metal plate was wider, the polymer instead of being extruded would be spread through the interface, contributing to the increase of joining area and potentially to the increase of mechanical strength. In addition, as in the triple spot welding the welds were performed very close to each other, there was overlap between the joining areas, which may have prevented a greater increase in joint strength. Still, the objective of this condition was to verify if multiple spot welding was feasible, which was demonstrated since the performance of multiple spot welding did not result in the separation of previous welds. Another aspect that could improve the performance of this type of welding is the study of the distribution of the multiple spot welds, which is suggested for future work.



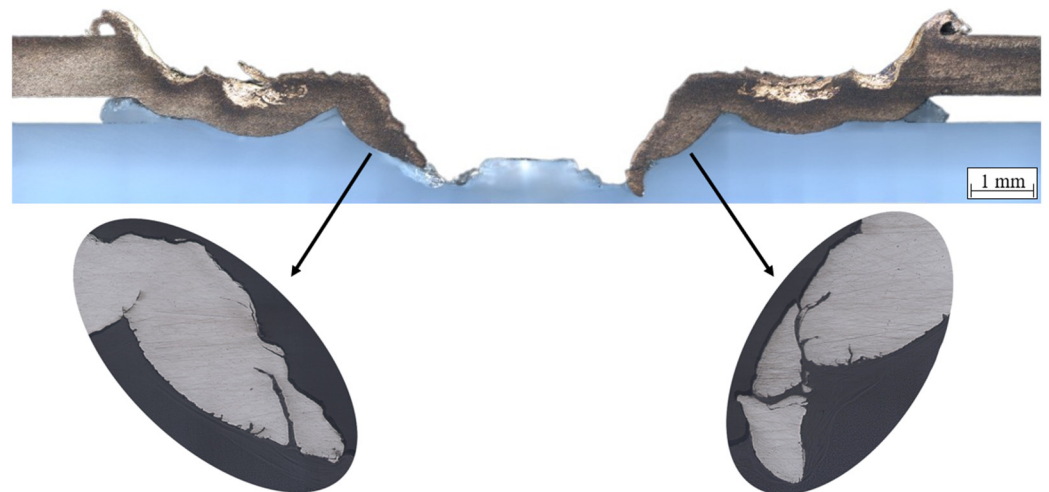
**Figure 9.** Surface finish of joints produced with (a) Single spot welding and (b) Triple spot welding.

### 3.4. Pinless Tool versus Conical Pin Tool

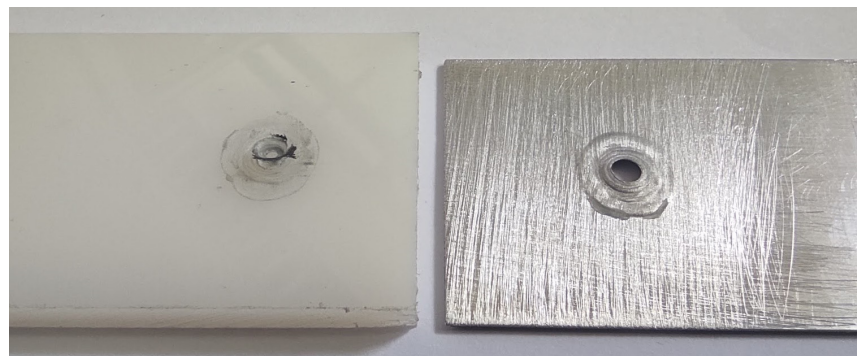
The last topic addressed in the current work was the comparison of the performance of a pinless tool and a tool with a conical pin. As demonstrated in the previous sections, the pinless tool managed to successfully join the aluminium and the polymer by FSSW for different conditions. However, to make the process competitive at industrial and commercial levels, the joint strength needs to be greater, which can be achieved by improving the mechanical interlocking mechanisms. In addition to the improvements that can be obtained by optimising the main welding parameters, such as the rotational speed, plunge depth or dwell time, the micro-mechanical interlocking may be improved with the improvement of surface treatments. On the other hand, the macro-mechanical interlocking mechanism is significantly influenced by the geometry of the tool. For this reason, a new tool was tested to understand if the proposed geometry could improve the mechanical performance of the welds. Welds produced with a pinless tool were compared to welds produced with a tool composed of a conical pin and a concave shoulder. This tool was chosen because it was intended to produce an irregular interface that would allow the aluminium to anchor well to the polymer. The cross-section obtained in the weld produced with this tool is provided in Figure 10.

Figure 10 shows that the aluminium was properly plunged into the polymer, in a wavy profile, indicating a good macro-mechanical interlocking. However, the weld produced with this condition resulted in a weak joint. Due to an excessive deformation of the aluminium, cracks were created throughout the deformed aluminium. Additionally, this tool promoted the rise of aluminium around the tool action zone, meaning that there was no contact between the materials in this region. When testing the strength of the weld produced with the conical tool (CN\_0.2\_10\_S), the specimens failed for a maximum force of about 700 N, as shown in Figure 8. This resulted in the separation of the plates by nugget pull-out, leaving remnants of aluminium in the polymer and vice versa, which can be observed in Figure 11. Although the mechanical tests have shown that this tool is not the most suitable for the current conditions, it cannot be said that the tool is not suitable for

metal-polymer joining by FSSW. One of the possible causes of bond failure when using this tool could be the use of excessively thin aluminium plates, as small deformations resulted in cracking of the metal plate, which may not be the case for thicker plates. For these reasons, it is suggested for future work the study of this tool with a conical pin for producing metal-polymer joining by FSSW with thicker aluminium plates. Regarding the joining of thin plates, the joining of 1 mm thick aluminium to PA6 by FSSW using a pinless tool was demonstrated in this work. In this sense, it is suggested for future work the study of the optimization of different welding parameters. Additionally, the study of new solutions for texturing the surface of the metal plate, with the aim of allowing the improvement of interlocking mechanisms, is also encouraged.



**Figure 10.** Cracking of the aluminium as a result of excessive tool penetration.



**Figure 11.** Surfaces of the bonding interface of welds produced with the conical pin tool after mechanical testing.

#### 4. Conclusions

Aluminium-PA6 joints were successfully produced by FSSW. The preliminary tests focused on the aluminium surface treatment and the tightening torque of the clamping frame made it possible to improve and standardise the welding conditions. This allowed us to study different parameters/conditions with greater reliability in the present research, which led to the following conclusions:

- The increase of plunge depth leads to an increase in mechanical strength up to the point where excessive penetration (0.5 mm) gives rise to rupture of the aluminium plate;
- Although the pore defects tend to increase with longer dwell times, an improvement in maximum load under tensile-shear testing resulted from the increase of the joining area. As a result, the increase of dwell time from 15 to 30 s resulted in the increase of joint strength from 1700 to 2100 N (an increment of about 24%);

- Triple spot welding was successfully demonstrated as the multiple welds do not result in the separation of previous welds, improving the mechanical performance when compared to single spot welds. The weld with the best mechanical behaviour was produced with multiple spot welding, which failed for a maximum load of about 2350 N (an increment of about 38%);
- The use of a more conventional tool with a conical pin and a concave shoulder result in the production of FSS welds between thin aluminium plates and PA6 with a lower strength (700 N) than those produced with a pinless tool. However, despite the lower strength of the weld produced with the tool with a conical pin, the interface of the materials was more irregular, indicating a better macro-interlocking between both materials. Therefore, despite not being suitable for the welding conditions of this study, the tool's potential for joints with thicker aluminium plates was demonstrated.

**Author Contributions:** Conceptualization, I.G., J.D.C., R.M.L. and A.M.A.; methodology, M.A.R.P., I.G. and R.M.L.; formal analysis, M.A.R.P.; investigation, M.A.R.P.; writing—original draft preparation, M.A.R.P., I.G., J.D.C., R.M.L. and A.M.A.; writing—review and editing, M.A.R.P., I.G., J.D.C., R.M.L. and A.M.A.; supervision, J.D.C., R.M.L. and A.M.A. All authors have read and agreed to the published version of the manuscript.

**Funding:** This research is sponsored by national funds through FCT-Fundação para a Ciência e a Tecnologia, under the project UIDB/00285/2020 and LA/P/0112/2020. The author Miguel A. R. Pereira is supported by the FCT through 2021.07543.BD fellowship.

**Data Availability Statement:** Data are contained within the article.

**Conflicts of Interest:** The authors declare no conflicts of interest.

## References

1. Lambiase, F.; Genna, S.; Kant, R. A procedure for calibration and validation of FE modelling of laser-assisted metal to polymer direct joining. *Opt. Laser Technol.* **2018**, *98*, 363–372. [[CrossRef](#)]
2. Amancio-Filho, S.T.; Bueno, C.; dos Santos, J.F.; Huber, N.; Hage, E. On the feasibility of friction spot joining in magnesium/fiber-reinforced polymer composite hybrid structures. *Mater. Sci. Eng. A* **2011**, *528*, 3841–3848. [[CrossRef](#)]
3. Cho, J.H.; Jae Kim, W.; Gil Lee, C. Texture and microstructure evolution and mechanical properties during friction stir welding of extruded aluminum billets. *Mater. Sci. Eng. A* **2014**, *597*, 314–323. [[CrossRef](#)]
4. Meng, X.; Huang, Y.; Xie, Y.; Li, J.; Guan, M.; Wan, L.; Dong, Z.; Cao, J. Friction self-riveting welding between polymer matrix composites and metals. *Compos. Part A Appl. Sci. Manuf.* **2019**, *127*, 105624. [[CrossRef](#)]
5. Pereira, M.A.R.; Galvão, I.; Costa, J.D.; Leal, R.M.; Amaro, A.M. Joining of Polyethylene Using a Non-Conventional Friction Stir Welding Tool. *Materials* **2022**, *15*, 7639. [[CrossRef](#)] [[PubMed](#)]
6. Thomas, W.M.; Nicholas, E.D.; Needham, J.C.; Murch, M.G.; Templesmith, P.; Dawes, C.J. Friction Stir Butt Welding. U.S. Patent No. 5460317, 24 October 1995.
7. Thomas, W.; Nicholas, E. Friction stir welding for the transportation industries. *Mater. Des.* **1997**, *18*, 269–273. [[CrossRef](#)]
8. Pereira, M.A.R.; Amaro, A.M.; Reis, P.N.B.; Loureiro, A. Effect of Friction Stir Welding Techniques and Parameters on Polymers Joint Efficiency—A Critical Review. *Polymers* **2021**, *13*, 2056. [[CrossRef](#)]
9. Pereira, M.A.R.; Galvão, I.; Costa, J.D.; Amaro, A.M.; Leal, R.M. Joining of Fibre-Reinforced Thermoplastic Polymer Composites by Friction Stir Welding—A Review. *Appl. Sci.* **2022**, *12*, 2744. [[CrossRef](#)]
10. Lambiase, F.; Balle, F.; Blaga, L.A.; Liu, F.; Amancio-Filho, S.T. Friction-based processes for hybrid multi-material joining. *Compos. Struct.* **2021**, *266*, 113828. [[CrossRef](#)]
11. Sun, Y.; Gong, W.; Feng, J.; Lu, G.; Zhu, R.; Li, Y. A Review of the Friction Stir Welding of Dissimilar Materials between Aluminum Alloys and Copper. *Metals* **2022**, *12*, 675. [[CrossRef](#)]
12. Yusof, F.; Miyashita, Y.; Seo, N.; Mutoh, Y.; Moshwan, R. Utilising friction spot joining for dissimilar joint between aluminium alloy (A5052) and polyethylene terephthalate. *Sci. Technol. Weld. Join.* **2012**, *17*, 544–549. [[CrossRef](#)]
13. Yusof, F.; bin Muhamad, M.R.; Moshwan, R.; bin Jamaludin, M.F.; Miyashita, Y. Effect of surface states on joining mechanisms and mechanical properties of aluminum alloy (A5052) and Polyethylene Terephthalate (PET) by dissimilar friction spot welding. *Metals* **2016**, *6*, 101. [[CrossRef](#)]
14. Lambiase, F.; Paoletti, A.; Grossi, V.; Ilio, A. Di Friction assisted joining of aluminum and PVC sheets. *J. Manuf. Process.* **2017**, *29*, 221–231. [[CrossRef](#)]
15. Lambiase, F.; Paoletti, A.; Grossi, V.; Genna, S. Improving energy efficiency in friction assisted joining of metals and polymers. *J. Mater. Process. Technol.* **2017**, *250*, 379–389. [[CrossRef](#)]

16. Lambiase, F.; Grossi, V.; Paoletti, A. Defects formation during Friction Assisted Joining of metals and semi crystalline polymers. *J. Manuf. Process.* **2021**, *62*, 833–844. [[CrossRef](#)]
17. André, N.M.; dos Santos, J.F.; Amancio-Filho, S.T. Evaluation of Joint Formation and Mechanical Performance of the AA7075-T6/CFRP Spot Joints Produced by Frictional Heat. *Materials* **2019**, *12*, 891. [[CrossRef](#)] [[PubMed](#)]
18. Goushegir, S.M. Friction spot joining (FSpJ) of aluminum-CFRP hybrid structures. *Weld. World* **2016**, *60*, 1073–1093. [[CrossRef](#)]
19. Goushegir, S.M.; dos Santos, J.F.; Amancio-Filho, S.T. Friction Spot Joining of aluminum AA2024/carbon-fiber reinforced poly(phenylene sulfide) composite single lap joints: Microstructure and mechanical performance. *Mater. Des.* **2014**, *54*, 196–206. [[CrossRef](#)]
20. Esteves, J.V.; Goushegir, S.M.; dos Santos, J.F.; Canto, L.B.; Hage, E.; Amancio-Filho, S.T. Friction spot joining of aluminum AA6181-T4 and carbon fiber-reinforced poly(phenylene sulfide): Effects of process parameters on the microstructure and mechanical strength. *Mater. Des.* **2015**, *66*, 437–445. [[CrossRef](#)]
21. Lambiase, F.; Paoletti, A. Mechanical behavior of AA5053/polyetheretherketone (PEEK) made by Friction Assisted Joining. *Compos. Struct.* **2018**, *189*, 70–78. [[CrossRef](#)]
22. Aliasghari, S.; Skeldon, P.; Zhou, X.; Ghorbani, M. Influence of PEO and mechanical keying on the strength of AA 5052 alloy/polypropylene friction stir spot welded joints. *Int. J. Adhes. Adhes.* **2019**, *92*, 65–72. [[CrossRef](#)]
23. Aliasghari, S.; Ghorbani, M.; Skeldon, P.; Karami, H.; Movahedi, M. Effect of plasma electrolytic oxidation on joining of AA 5052 aluminium alloy to polypropylene using friction stir spot welding. *Surf. Coat. Technol.* **2017**, *313*, 274–281. [[CrossRef](#)]
24. Aliasghari, S.; Skeldon, P.; Zhou, X.; Hashimoto, T. Effect of an anodizing pre-treatment on AA 5052 alloy/polypropylene joining by friction stir spot welding. *Mater. Sci. Eng. B* **2019**, *245*, 107–112. [[CrossRef](#)]
25. Asadollahi, M.; Jabbari, N.; Nakhodchi, S.; Salimi, H.; Khodaparast, H.H. Analysis of tensile-shear strength of single and multi-friction stir spot welding joints under fixed welding process conditions. *Proc. Inst. Mech. Eng. Part C J. Mech. Eng. Sci.* **2020**, *234*, 4893–4904. [[CrossRef](#)]

**Disclaimer/Publisher's Note:** The statements, opinions and data contained in all publications are solely those of the individual author(s) and contributor(s) and not of MDPI and/or the editor(s). MDPI and/or the editor(s) disclaim responsibility for any injury to people or property resulting from any ideas, methods, instructions or products referred to in the content.